Numerical and Experimental Study of Winglet Effect with Different Cant Angles

Dr. Anmar H. Ali
lecturer
aha_has@yahoo.com
Ammar G. Khadum
ammarghany@yahoo.com
Engineering College
Baghdad University\Iraq

Abstract

The present work aims to investigate the aerodynamic characteristics of the winglet cant angle of Boeing 737-800 wing numerically and experimentally. The wing contain two swept angles 38.3° and 29.13° respectively, taper ratio 0.15 and aspect ratio 8.04. The wing involves three types of airfoils sections. Four cant angles for blended winglet have been considered (0°, 34°, 60°, 83.3°). The winglet has been analyzed to find the best cant angle for the wing without and with winglet. These models have been tested theoretically at Reynolds number of 2.06 $x10^6$ in order to study the winglet aerodynamic characteristics which consist of coefficient of Drag, coefficient of lift and Lift to drag ratio, pitching moment coefficient and bending moment coefficient for (0°, 2°, 4°, 6°, 8°, 10°) angles of attack. SOLIDWORK 2016 software, was used to design the geometry of the wing and winglet. ANSYS FLUENT 17.0 in three dimensions with (k - ε) turbulent model was used to solve the governing equations. The experimental tests were carried out in an open low subsonic wind tunnel of 70cm × 70cm ×150cm test section at Reynolds number of 4.33 $x10^5$. The experimental lift, drag forces and pitching moment measurement were considered by three component balance device at different angles of attack. The results show that 34° cant angle is the best angle, at which 2-3% increase in lift coefficient, 2-3.9% decrease in drag coefficient, 3.5-6% increase in pitching moment coefficient and 3-6.6% increase in lift to drag coefficient by using blended winglet. Good agreement between the experimental and computational results are shown.

Key Words: Aerodynamic characteristics, Boeing 737-800 wing, Winglet, Cant angle

1. Introduction

The price of fuel is an important factor in the civil aircraft. Engineers are always working to optimize the aircraft. In the field of civil aviation, the best advantage in the recent years is the wingtip device. In early 1970, Richard T. Whitcomb with a team work including Jacobs and Stuart G. Flechner were studied trailing vortices in the research centre of NASA's

Langley. They proved the acceptability of winglet idea in the state of reducing the induced drag. Whitcomb's studies were based on NASA flight-tested KC-135 aircraft in the Research Centre of Dryden Flight at 1979-1980. The results of the research had been proved a possibility to increase 7% aircraft's range at cruise speed.

It is found that when the drag of the Boeing 747-400 was reduced by 2.5%, a 9.5 tons at take-off could be saved Lambert Dimitri, 2008. The performances well improved for the Boeing 737, and 757-200, by using a blended winglet, which save about two hundred million dollars in fuel cost per aircraft when the wing efficiency increased by 2%, Reddy et al. 2014. Winglet can be defined as a vertical extension fix at the wing tips. These devices increase the aircraft efficiency by reducing the induced drag which is being caused by the vortices generated at the wing tip. Atique et al. 2015. Many researches and authors had studied the winglet cant angles for different wings and different winglets. Abdelghany, et al. 2016 investigated a numerical analysis of a three-dimensional wing with winglets at various cant angles 0°, 30° and 45°(the angles measured from the vertical axes), the wing with different types of winglets (blended, finlet and bird like winglet) was studied by Dwivedi et al. 2016 numerically and experimentally, also, they found that 45^o cant angle was the best angle. For wing with blended winglet Alka Sawale, et al. 2017 investigated the increment in the lift force and decrement in the drag force by using a blended winglet attached the end of the wing with various cant angles (15^o, 30^o, 60^o). The angles were measured from the horizontal axes). The results showed an increase in L/D increase and a decrease in the drag force.

In the present work, numerical and experimental investigation are performed to analyse the winglet performance for the Boeing 737-800 wing by changing the cant angle.

2. Mathematical model

The wing and winglet geometry have been described in this section. The details of configurations cross-sectional airfoils, aspect ratio, taper ratio, dihedral angles……etc., are presented as follows.

2.1 Wing Geometry

The wing model of Boeing 737-800 airplane is used in this work, the wing involves three types of airfoil sections, root airfoil (b737a), midsection airfoil (b737c), tip airfoil (b737d) Atique et al. 2015. The wing has two leading edge sweep back angles (38.3^o and 29.13^o), taper ratio of (0.159), aspect ratio of (8.04), span length of (15m) and dihedral angle (6^o). The wing with winglet was modeled by a SOLIDWORKS Design

Modular, where the dimensions are divided by the length of root chord. In figure 1 shows the top and side view of the wing.

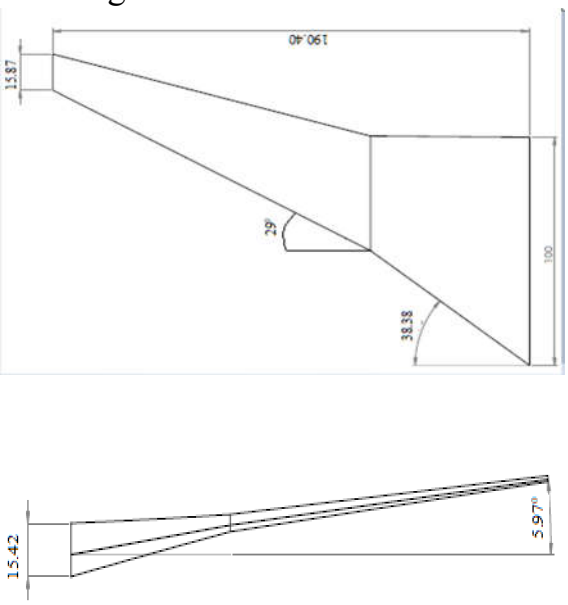

Fig. 1 Top and side views of wing model (all dimensions in centimeter)

2.2 Winglet Geometry

A blended winglet is attached to the wing with span 3.59m, root chord1.25m, taper ratio 0.36m and cant angle 34^o as shown in the figure 2. The winglet is modelled by an airfoil section of (b737d), all dimensions are divided by the length of root chord of the wing. Four cant angles of the winglet have been studied (0^o, 34^o, 60^o, 83.3^o) as shown in the figure 3, at different angles of attack as 0^o, 2^o, 4^o, 6^o, 8^o, 10^o.

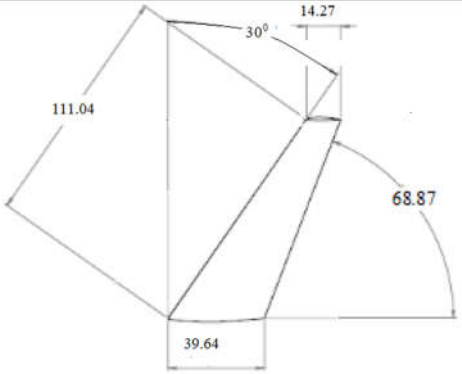

Fig. 2 Top view of winglet model

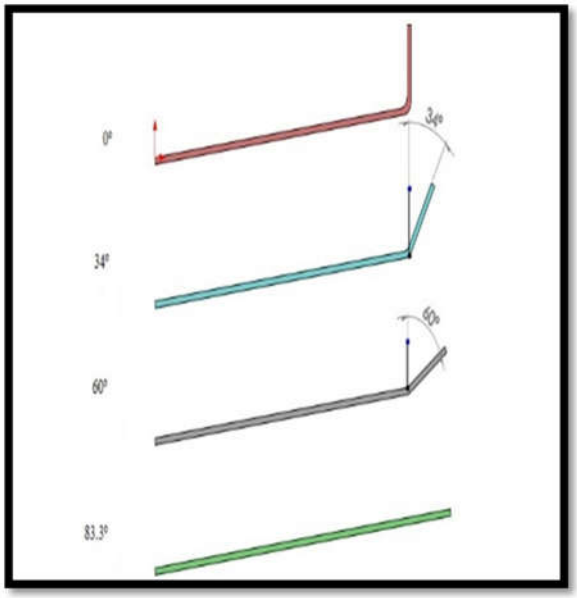

Fig. 3 Types of winglet cant angle

3. Computational Approach

The governing equations are solved by the FLUENT ANSYS software which consists of three main steps. The first is the pre-processing which are a 3-D geometry modeling by using SOLIDWORKS Software. The second step is processing the governing differential equations for air flow around the wing without and with winglet by ANSYS FLUENT solver by utilizing a Finite Volume Method

and Finally, the post-processing step in which the aerodynamic characteristics coefficient of lift (C_L), coefficient of drag (C_D) and the Lift-to-Drag ratio (L/D) at different angles of attack and specified Re are evaluated. The methodology is presented in the following sections.

The following assumptions were used by the software package for the working fluid;

1. Steady flow
2. Three-dimensional flow about the geometry.
3. Subsonic and incompressible, (M<0.3).
4. Neglecting the body forces.
5. Neglecting heat transfer effects with the physical properties are constants.
6. Turbulent flow with (k-ε turbulence model).
7. The fluid is considered as a continuum and Newtonian.

The governing equations used by the software package are the steady incompressible for each of continuity and momentum equations:

$$\frac{\partial}{\partial x_i} u_i = 0 \quad \text{.................................} \quad (1)$$

$$u_j \frac{\partial u_i}{\partial x_j} = -\frac{1}{\rho} \frac{\partial P}{\partial x_i} + \frac{\partial}{\partial x_j}\left(\vartheta \frac{\partial u_i}{\partial x_j} - u_i u_j\right) \text{..} \quad (2)$$

The system geometry in the present work is a three dimensional with Cartesian coordinates, where the z-direction represents the air flow direction, the system geometry consists of rectangular domain and this rectangular domain contains a wing model. The size of the computational domain chosen to extends one of wing root chord length C in front of the model and 3.25 C behind the trailing edge of the wing, to simulate the wake region of the wing. The distance between the upper boundary and the wing is set to 2 C. The distance between the lower boundary and the wing is set to 1.5 C. The distance between the tip of the wing and the side wall of the domain is set to one of wing root chord, Atique et al. 2015. The computational domain is formed with appropriate dimensions as shown in figure 4.

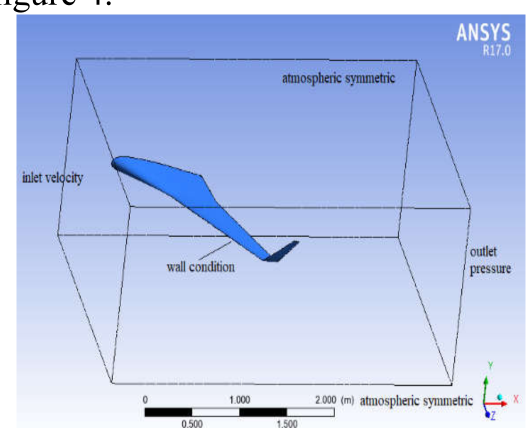

Fig. 4 Computational domain dimensions and boundary conditions of the wing with winglet.

A mesh is defined by dividing the domain and model geometries into simple shapes of small units, using tetrahedral meshing with finer sizing near the model to evaluate the flow

characteristics accurately. The grid was generated. The number of cells has been examined between 5,000,000 cells to 7,000,000 cells. The chosen grid is 6,270,000 cells; which selected through grid independence test (see figure 5).

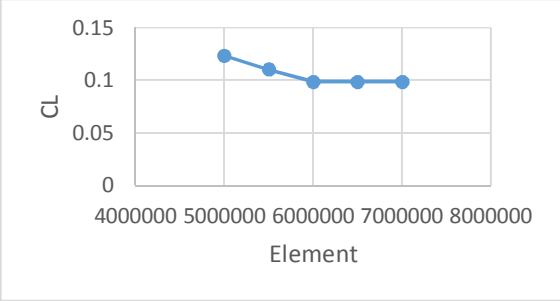

Fig. 5 Grid independence test

The Mesh of domain with 3D wing model is shown in the figure 6. The smallest cells are generated near the adjacent surface of the wing, and the larger cells are located near the boundary domain (see figure 6).

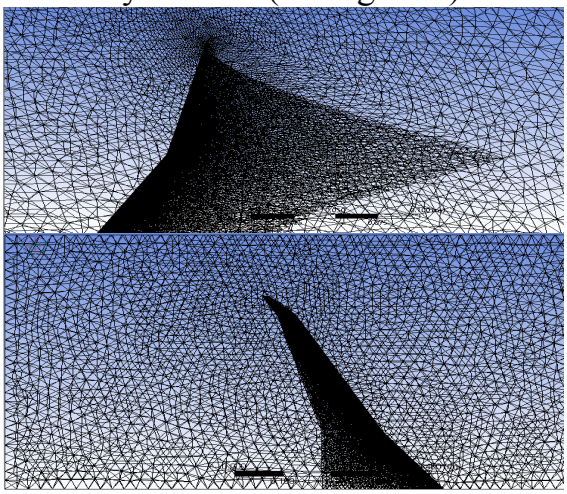

Fig. 6 Mesh of domain with wing model

4. Experimental Work

All the present experimental work were performed in a low-speed, open circuit wind tunnel shown in figure 7, The dimensions of the test section are (0.7m × 0.7m × 1.5m). The design and construction of this tunnel was made completely by a number of faculty staff of the Department of Mechanical Engineering at the College of Engineering University of Baghdad. Hussain et al. 2011 and Hussain and Ali, 2014**.**

Fig. 7 Low speed wind tunnel

The designed winglet and the Boeing (737 -800) wing were manufactured with reduced size of (1/13) and tested in wind tunnel. The aerodynamic characteristics and flow visualization were measured using a modified three-component balance device. The tests consist of wing with winglet and clear wing at different angles of attack. The coefficients are calculated for final results to be compared with numerical results.

The wing and winglets manufactured by Perspex. After that, the surface was polished and softened until it became smooth and then was painted with thermal paint as shown in the figure 8. The winglet was connected to the wing by small screws. Then a base was built to hold the wing with a shaft to connect the wing into a

three component balance, as shown in the figure 9 and figure10.

Fig. 8 Wing model

Fig. 9 The model in the test section

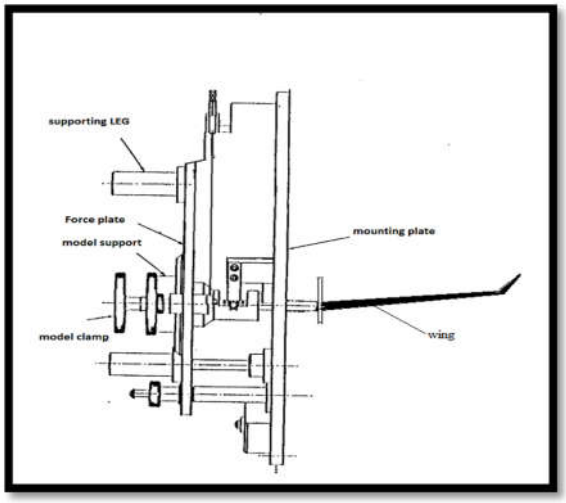

Fig. 10 Three component balance and wing (side veiw)

Figure 11 shows the modified three component balance which is used with the present wind tunnel to find the force and moments of the model. It consists of three actuators, the drag actuator which acts in the horizontal direction and passes through the axis of the model support, while other two lift actuator acts vertically through a points that are in the same level and equidistant horizontally from the vertical axis. The distance between the fore and aft actuator is (150 mm) and the sum of the forces in these load cells gives the lift on the model in Newton while the difference between them multiplied by (0.075 m), gives the pitching moment in Newton–meter.

The three component balance has been accurately calibrated to obtain the precise constant for lift and drag cables. Connect the load cell in the Digital Weighing Indicator SI 480 shown in the figure 11.

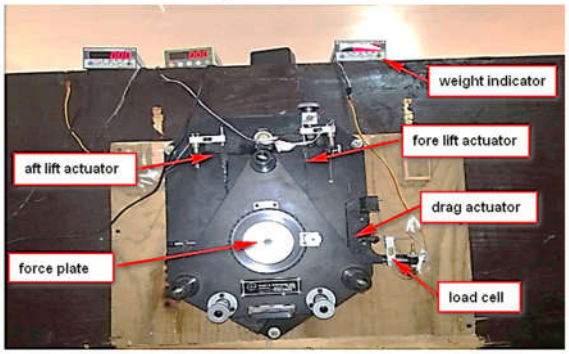

Fig. 11 Three component balance

The calibration was done against dead weight with the use of calibrating arm, which provided with a pivoted

loading link from which dead weight may be hung and located either at the end of the rod or in two alternatives position each displaced (0.15) from the line center of the rod calibration should be carried out with the balance mounted on the tunnel, shown in the figure 12, 13

Fig.12 Calibration of lift force

Fig.13 Calibration of drag Spring

The experimental calculations for the wing with and without winglet are given below;

Total lift = L = (L1+L2) × 9.81 (N) ……..…….. (3)

Total drag = D =D1 × 9.81 (N) …….. (4)

Pitching moment = M = (L2 × 0.075 – L1 × 0.075) × 9.81 (N.m) …. (5)

The expression for the lift coefficients, drag coefficients and the moment coefficients are given by

$$C_L = \frac{L}{\frac{1}{2}\rho_\infty v_\infty^2 S} \quad \text{……..} \quad (6)$$

$$C_D = \frac{D}{\frac{1}{2}\rho_\infty v_\infty^2 S} \quad \text{……..} \quad (7)$$

$$C_M = \frac{M}{\frac{1}{2}\rho_\infty v_\infty^2 S c_{ref}} \quad \text{……..} \quad (8)$$

The Pitot-Static tube and Micro-Manometer were used to measure the pressure at inlet of test section. The free stream air velocity was 30 m/s.

5. Results and Discussions

5.1 Theoretical Results

Four models of cant angles (0^o, 34^o (reference angle), 60^o, 83.3^o), are used as shown in the figure 3. All the previous geometric parameters are considered constant when variation of cant angle is considered.

The Lift coefficients for various cant angles of different angles of attack are presented in figure 14. It is obvious that, when the cant angle of the winglet increased, the wetted area of the wing is increased causes the lift

coefficient to increase. But for larger cant angles a reduction in the lift coefficient are noticed. The lift maximized when the cant angle is 83.3° which be in horizontal extension of the wing tip.

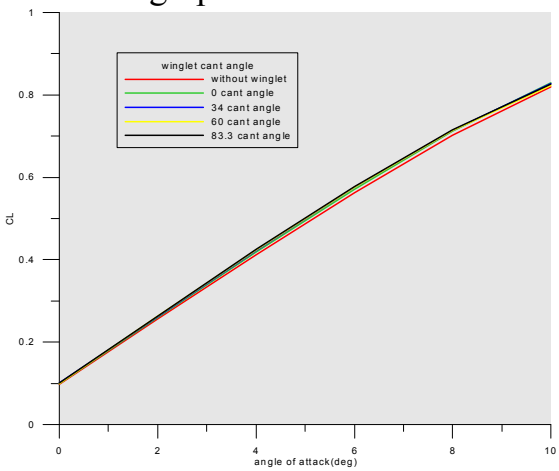

Fig.14 Lift coefficient versus angle of attack for wing with winglet at different cant angle

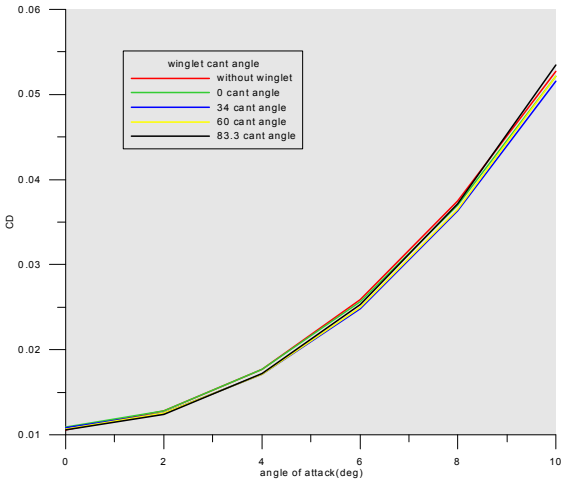

Fig. 15 Drag coefficient versus angle of attack for wing with winglet at different cant angle

The drag coefficient for various winglet cant angle at different angles of attack is shown in the figure 15. It is observed that the drag coefficient increases with increasing the angle of attack; at 0° degree angle of attack the effect of wing with different winglet cant angle is not important because the induced drag is minimum value and the frictional drag is dominant this angle. At high angles of attack the induced drag is increased making the total drag to be large. The minimum reduction in drag coefficient is found at 0° angle of attack while the maximum at 34° for different angles of attack.

The pitching moment coefficient for various cant angles at different angles of attack is presented in figure 16. It is obvious that when the cant angle increment causes an increase in the pitching moment, therefore the stability of the wing is increased. The wing with winglet at cant angle 83.3° which is considered at tip extension becomes more stable than others.

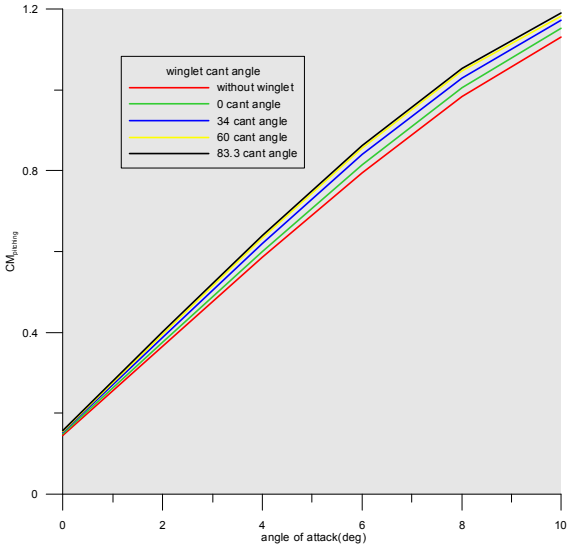

Fig. 16 Pitching moment coefficient versus angle of attack for wing with winglet at different cant angle

Figure 17 indicates the bending moment coefficient relation with a variation of the angle of attack for different models of cant angles. It is obvious that the increasing of cant angle causes an increase in the wetted-area of the wing with winglet, the reduction in the bending moment is considerably greater for high cant angles, which indicates that the horizontal extension is not favorable in designing the wing of airplane due to increasing the bending moment. Also the weight increased causes to increase the bending moment at the root and needing for more reinforcement.

The lowest bending moment coefficient is at 0° cant angle of 2.58003% as compared to wing without winglet for different angles of attack. The highest bending moment coefficient is at 83.3° cant angle about 6.64871% as compared to wing without winglet for different angles of attack.

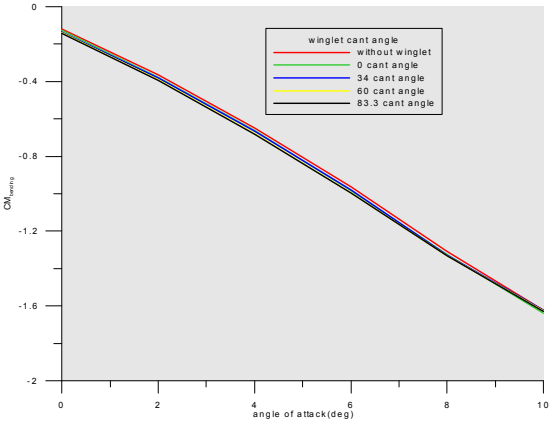

Fig. 17 Bending moment coefficient versus angle of attack for wing with winglet at different cant angle

The ratio C_L/C_D is shown in the figure 18, wing with winglet at cant angle of 34° has the highest lift-to-drag ratio, any increment more than 34° causing a decrease in the ratio of C_L/C_D.

The previous aerodynamic characteristics show that the increasing of the cant angles causes an increase in the coefficients as a result of increasing the wetted area of the wing. This increasing does not necessary be preferable due to bending coefficient increase which causes an additional load consideration.

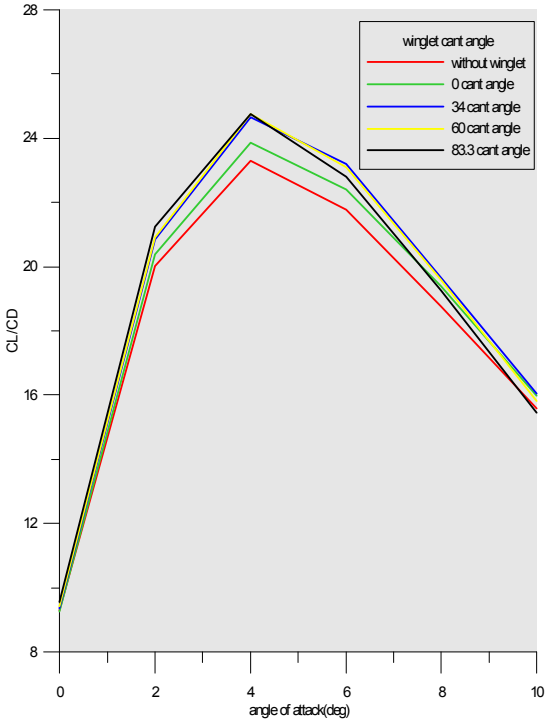

Fig. 18 Lift to drag ratio versus angle of attack for wing with winglet at different cant angle

The Streamlines in the wake region at (0°, 34°, 60°, 83.3°) respectively of winglet are presented in figure 19, 20, 21 and 22 at 4° angle of attack.

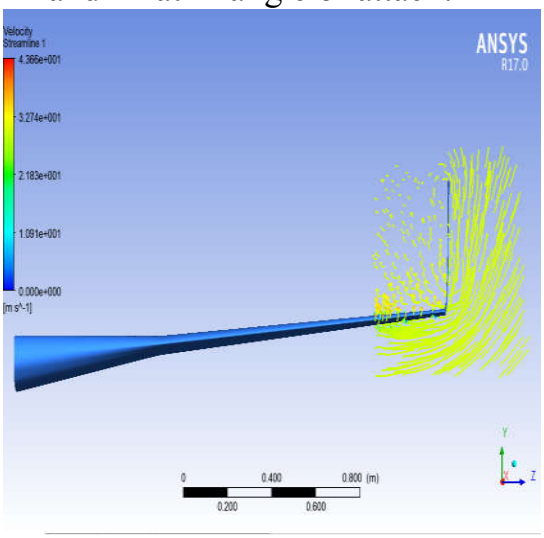

Fig. 19 Velocity vector in wake region at 0° cant angle of winglet

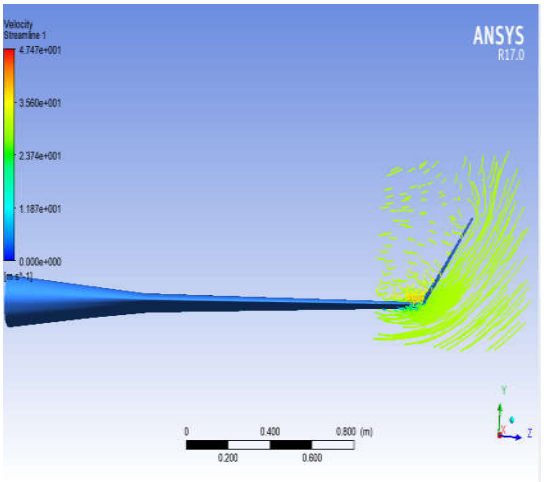

Fig. 20 Velocity vector in wake region at 34° cant angle of winglet

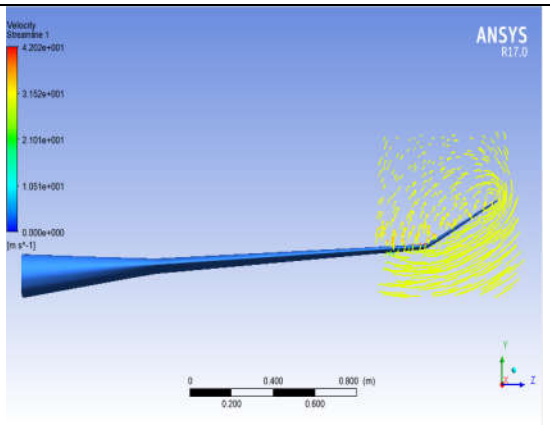

Fig. 21 Velocity vector in wake region at 60° cant angle of winglet

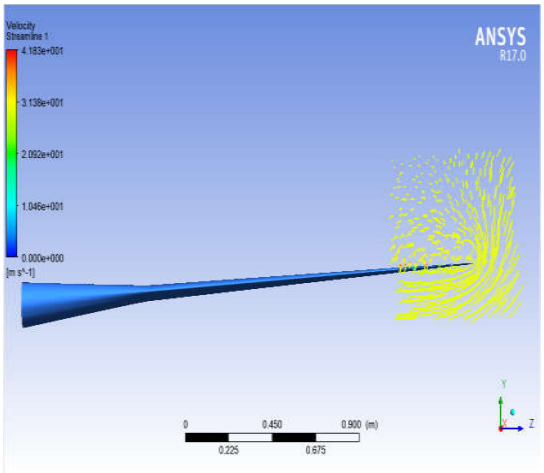

Fig. 22 Velocity vector in wake region at 83.3° cant angle of winglet

From the results, the determination of optimum winglet cant angle was found to be equal to 34° which has a minimum value of drag coefficient, higher lift to drag coefficient and an increase in the bending moment less than 5%. So it gives an optimum aerodynamics performance.

5.2 Experimental Results

To cover the investigated parameters in the experimental part of

this work, more than 12 test runs were performed for Boeing 737-800 wing without and with winglet. The lift force, drag force and pitching moment along the wing without and with winglet were measured by the three component balance to find the lift coefficients, drag coefficients, and pitching moment coefficients. The required velocity in each test run was found by measuring the dynamic pressure at the inlet of the test section. The Reynolds number where the experiments have been performed is 4.33 x10^5. The forces data were recorded; and the data were collected for different angles of attack (0^o, 2^o, 4^o, 6^o, 8^o, 10^o).

Figure 23; shows the experimental lift coefficient along the wing with and without winglet for different angles of attacks. It is obvious that the lift coefficient increased with increasing the angles of attack in approximately linear relation. The wing has been enhanced by adding a winglet as shown in the figure, which is identified in the previous theoretical work. The results show an increasing of lift coefficient about 0.16% to 3.6% as compared to wing without winglet for different angles of attack. The effect of winglet is increased as the angles of attack increased except at high angle of attack, this increment has been reduced as shown in the figure.

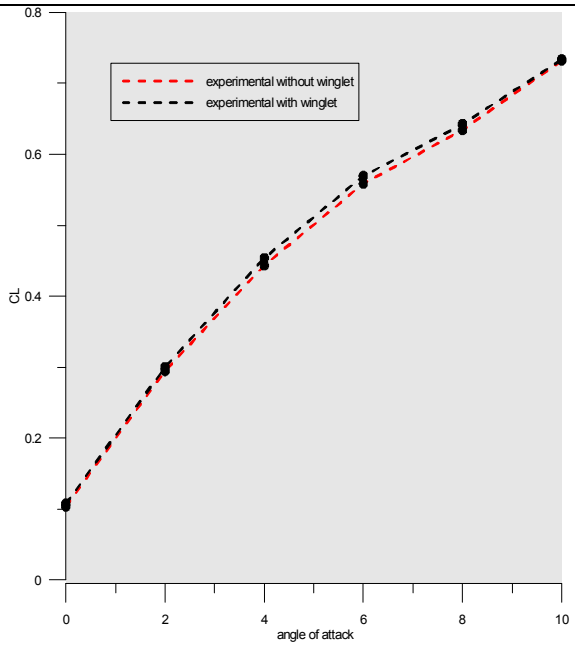

Fig. 23 Experimental lift coefficient versus angles of attack for wing with/without winglet at Re= 4.33x10^5

The experimental drag coefficient for different angles of attack of wing with and without winglet is presented in figure 24. As discussed previously, an increase in the drag coefficient is shown in the figure with parabolic behavior. The drag coefficient in the experimental results decreases for different angles of attack when the winglet is added at the tip end of the wing. This reduction is about 0.47% to 2.02%.

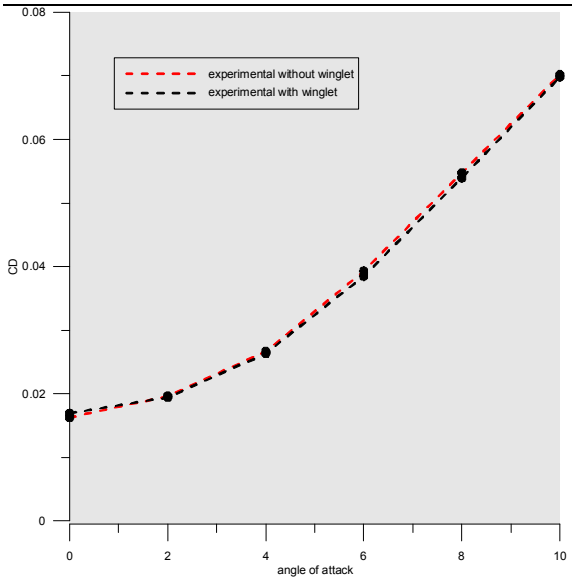

Fig. 24 Experimental drag coefficient versus angles of attack for wing with/without winglet at Re= 4.33x10^5

The pitching moment coefficient is presented in figure 25, for different angles of attack. When the winglet is added, the wing becomes more stable. An increasing in the pitching moment coefficient is noticed as compared with experimental wing without winglet for different angles of attack by a percentage range of 0.91% to 7.27%.

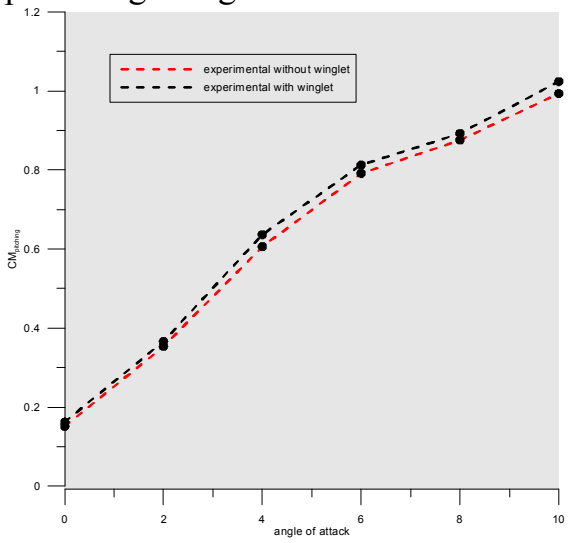

Fig. 25 Experimental pitching moment coefficient versus angles of attack for wing with/without winglet at Re= 4.33x10^5

figure 26 show the experimental ratio of lift to drag coefficient for the wing with and without winglet at different angle of attack. It is clear that C_L/C_D has the same effective angle of attack which obtained by theoretical results. The increased percentages of lift to drag ratio in the experimental results are 0.63% to 4.07%.

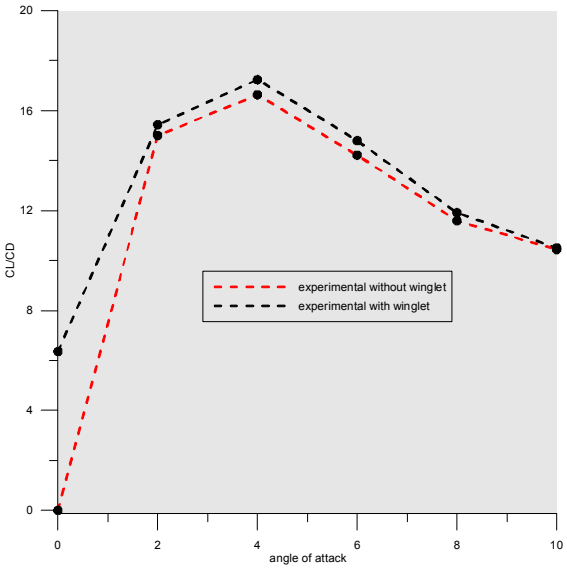

Fig.26 Experimental lift to drag ratio versus angles of attack for wing with/without winglet at Re= 4.33x10^5

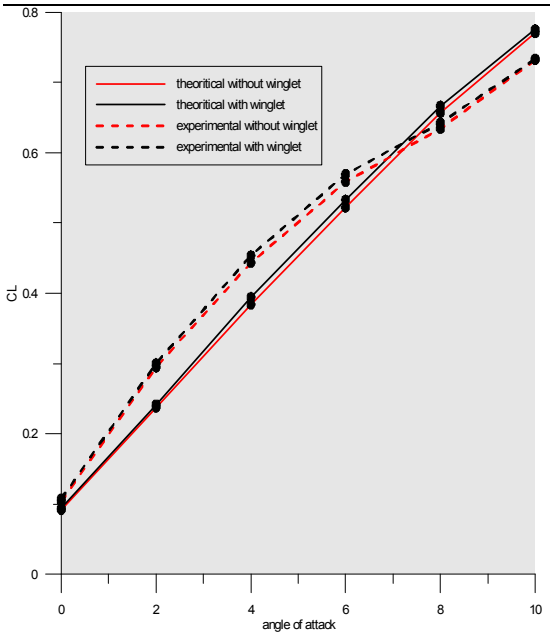

Fig.27 Theoretical and experimental verifications of lift coefficient versus angles of attack for wing/winglet Re= $4.33x10^5$

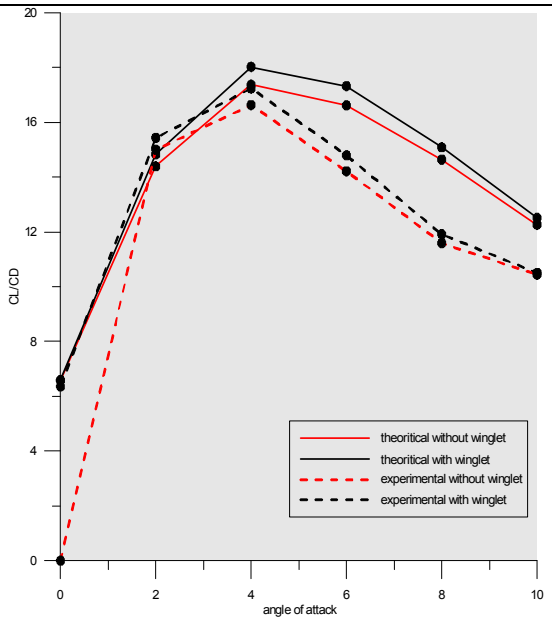

Fig.28 Theoretical and experimental verifications of lift to drag Coefficient variation versus angles of attack for wing with/without winglet at Re= $4.33x10^5$

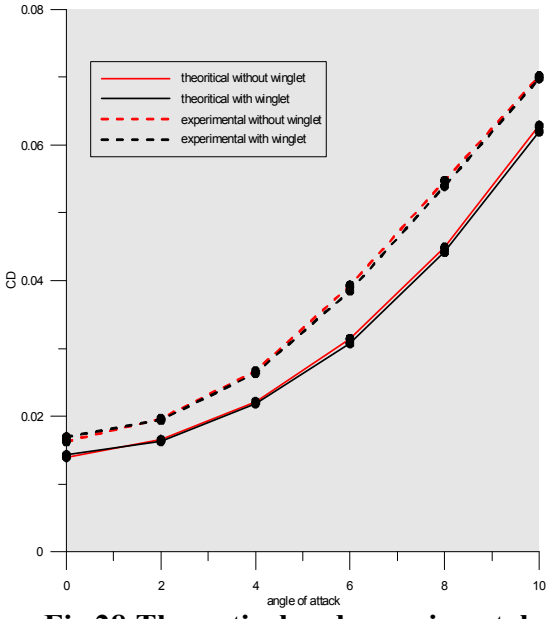

Fig.28 Theoretical and experimental verifications of drag coefficient versus lift coefficient for wing/winglet at Re= $4.33x10^5$

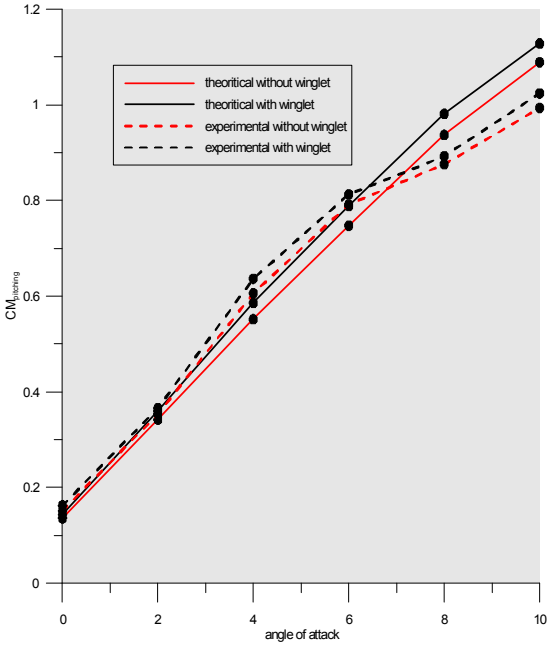

Fig.30 Theoretical and experimental verifications of pitching moment coefficient variation versus angles of attack for wing with/without winglet at Re= $4.33x10^5$

6. Conclusions

- The highest averages lift coefficient difference percentage as compared to wing without winglet is 2.20763%for 83.3^o cant angle.
- The lowest reduction of drag coefficient percentage as compared to wing without winglet is at 34^o cant angle -2.20763%.
- that a stable pitching moment for the wing with winglet at 83.3^o cant angle which increased about 7.9752%as compared to wing without winglet for whole angles of attack
- that the lowest decreasing in bending moment coefficient averages percentage is at 34^o cant angle 3.37821% as compared to wing without winglet
- the wing is more efficient at 34^o cant angle with increasing averages percentage equal to 4.251501%in the C_L/C_D ratio when compared with wing without winglet for different angles of attack
- The optimum winglet cant angle was found to be equal to 34^o which has a minimum value of drag coefficient, higher lift to drag coefficient and an increase in the bending moment less than 5%. So it gives an optimum aerodynamics performance.

Notation

L: lift force (N)
L1, L2: Aft and fore lift actuator (Kg)
D1: Drag actuator (Kg)
D: drag force (N)
M: pitching moment (N.m)
p_∞: density of free stream(Kg/m^3)
v_∞: velocity of free stream (m/s^2)
S: projected area (m^2)

References

- Abdelghany, E. E. Khalil, O. E. Abdellatif and G. ElHarriri, "Winglet Cant and Sweep Angles Effect on Aircraft Wing Performance", 17 MP 258th Int. AMME Conference, 19-21 April, 2016.
- Alka S., MD Khaleel, S. Jaswanth, "Desgin and Analysis of Winglet", International Journal of Civil Engineering and Technology (IJCIET), V. 8, Issue 5, May 2017, PP. 842- 850, Article ID:IJCIET_08_05_093.
- Atique, Md. Abdus S., Asif S.N., Nafisa N. P. and Shuvrodeb B., "Aerodynamics of Winglet: A Computational Fluid Dynamics Study", Global Science and Technology Journal, Vol. 3. No. 1. March 2015 Issue.
- Dwivedi, Patil M. P., "Design and Aerodynamic Analysis of Different Winglet", (IJIET), V 7, Issue 2, 2 August 2016.

- Hussain H. Al-Kayiem, Chelven .A. K. A. K., "An Investigation on the Aerodynamic Characteristics of 2-D Airfoil in Ground Collision", Journal of Engineering Science and Technology, Vol. 6, No. 3, P.P.369 – 381, 2011.
- Hussain I. Y. and Ali A. H., "Calibration of Low-Speed Wind Tunnel (LSWT) Test Section", Baghdad University Engineering Journal, Dossier No. ME-576.
- Lambert Dimitri, "Numerical Investigation of Blended Winglet Effects on Wing Performances", Aalborg University, Denmark, June 2008. DK-9220, FACE-10.
- Sohail Reddy, Shanae P., Abraham N., "Design, Analysis and Multi-Objective Constrained Optimization of Multi-Winglets", Florida International University FIU, DOI: 10.1051/C EDP Sciences, 2014.

دراسة نظرية وعملية لتأثير الجنيح الطرفي مع زوايا ميلان مختلفة

د. انمار حامد علي
مدرس
عمار غني كاظم
قسم الهندسة الميكانيكية / كلية الهندسة
جامعة بغداد

يهدف هذا البحث الى دراسة الخصائص الايروديناميكية لزاوية ميلان الجنيح الطرفي لجناح طائره بوينك (800- 737) نظريا وعمليا. يحتوي الجناح على زاويتي تراجع (38.3^{o}-29.13^{o}) على التوالي, طرف مستدق بنسبه 0.159 ونسبه باعيه قيمتها 8.04. يتضمن الجناح ثلاث مقاطع مطيار. أربع زوايا عن الافق للجنيح الطرفي نوع (blended) والتي هي (83.3^{0}, 60^{0} , 34^{0}, 0^{0}).

تم تحليل الجنيح الطرفي لأيجاد افضل العوامل لشكل الجناح دون رفع الجنيح الطرفي وقد تم اختيار هذه العوامل نظريا عند رقم رينولد ($Re= 2.06\ x10^{6}$) من اجل دراسه الخصائص الهوائيه للجنيح الطرفي والتي تحمل معامل السحب , ومعامل الرفع ونسبه الرفع الى السحب , معامل عزم التأرجح , ومعامل عزم الانحناء لزوايا هجوم(0, 2,4,6,8,10) . أستخدم برنامج SOLIDWORK 2016 لتصميم وهندسه شكل الجناح والجنيح الطرفي وبرنامجANSYS FLUENT ثلاثي الابعاد مع نموذج اضطرب (k - ε) لحل المعادلات الحاكمه .وقد تم اجراء الاختبارات العمليه في نفق هوائي منخفض السرعه ذي مقطع اختبار (cm 70cm * 70 *150cm) عند رقم رينولد $Re = 4.33\ x10^{5}$.تم قياس قوة الرفع العملي والكبح وعزم التأرجح تم قياسها عن طريق جهاز ثلاثي التوازن عند زوايا هجوم مختلفه. اظهرت النتائج ان الجنح الطرفي , المرجعي له افضل معاملات شكل.(3 - 2 %) زياده في معامل الرفع , وانخفاض بنسبه(3.9 – 2 %) في معامل السحب , وزياده (6- 3.5%) في معامل عزم التأرجح, (6.6- 3%)زياده في نسبه معامل الرفع الى السحب بأستخدام الجنح الطرفي نوع (blended) . وقد اظهرت النتائج وجود توافق جيد بين النتائج العمليه والنظرية.